Hydrodynamic description of the adiabatic piston

M. Malek Mansour,[1] Alejandro L. Garcia,[2] and F. Baras[3]

[1]*Universite Libre de Bruxelles, 1050 Brussels, Belgium*
[2]*Department of Physics, San Jose State University, San Jose, California, USA*
[3]*Université de Bourgogne, LRRS, F-21078 Dijon Cedex, France*

A closed macroscopic equation for the motion of the two-dimensional adiabatic piston is derived from standard hydrodynamics. It predicts a damped oscillatory motion of the piston towards a final rest position, which depends on the initial state. In the limit of large piston mass, the solution of this equation is in quantitative agreement with the results obtained from both hard disk molecular dynamics and hydrodynamics. The explicit forms of the basic characteristics of the piston's dynamics, such as the period of oscillations and the relaxation time, are derived. The limitations of the theory's validity, in terms of the main system parameters, are established.

PACS number(s): 05.70.Ln, 05.40.−a

I. INTRODUCTION

Consider an isolated cylinder with two compartments, separated by a piston. The piston is free to move without friction along the axis of the cylinder and it has a zero heat conductivity, hence its designation as the *adiabatic piston*. This construction, first introduced by Callen [1], became widely known after Feynman discussed it in his famous lecture series [2]. Since then it has attracted considerable attention [3–5]. For a sufficiently large piston mass, the following scenario describes the evolution of the system [6,7]. Starting from a nonequilibrium configuration (i.e., different pressures in each compartment) the piston performs a damped oscillatory motion. The oscillations eventually die out and the system reaches an intermediate state of "mechanical equilibrium," with equal pressure on each side of the piston, but different densities and temperatures (see Fig. 1). On a second (much longer) time scale, a slow relaxation towards the "full thermodynamic equilibrium" state with equal temperatures and densities takes place (Fig. 2).

This construction is interesting for two reasons. First, the second stage of the relaxation (e.g., $t > 5 \times 10^5$ in Fig. 2) provides a microscopic example of a so-called Brownian motor [8,9]: the fluctuations of the momentum exchanges between piston and particles establish a microscopic "thermal" contact between the two compartments. As a result, a slow effective heat transfer and a concomitant systematic motion of the piston appears, until eventually full thermodynamic equilibrium is reached. Both compartments are then at equilibrium, with the same temperature and pressure.

Second, there is an apparent paradox regarding the thermodynamic limit, $N \to \infty$, $V \to \infty$, $N/V = n < \infty$, where N represents the total number of particles, V the volume of the cylinder, and n the global number density of the fluid. The piston motion arises from a pressure difference ΔP exerted by the fluid on each side of it. The resulting acceleration a_p is then given by $a_p = \Delta P S / M$, where M and S denote the piston mass and surface, respectively. In the thermodynamic limit, the behavior of the piston greatly depends on how we take this limit at the piston level. The natural way is to fix once and for all the ratio M/S (i.e., fixed piston thickness) and to

consider the limit $M \to \infty$, $S \to \infty$ with finite, nonzero piston acceleration a_p, so that the first stage of the evolution remains essentially unchanged. The piston thus eventually reaches the mechanical equilibrium state where each compartment is practically at thermodynamic equilibrium with different temperatures and densities. It then follows from basic principles of equilibrium statistical mechanics that intensive state variables such as temperature, pressure, and density tend to their (most probable) macroscopic values in the thermodynamic limit, i.e., their fluctuations vanish [10]. As a result the microscopic "thermal" contact between the two compartments and the resulting heat transfer also vanish. This in turn implies that the second stage of the relaxation simply disappears so that the intermediate mechanical equilibrium state becomes the genuine final equilibrium state of the system (MD simulations illustrating this behavior are presented in Sec. II, Fig. 3). As noticed by several authors [11–13], the application of the maximum entropy criterion to predict this equilibrium state subsequently runs into trouble if the thermodynamic limit is taken prior to the $t \to \infty$ limit. The physical reason appears to be the degeneracy of the mechanical equilibrium state: any state with the two compartments separately at equilibrium, with the same pressure and the piston at rest, is a possible equilibrium state. Equality of temperatures need not be achieved, because of the adiabatic property of the piston, leading to the paradoxical conclusion that in the thermodynamic limit the final state is not unique.
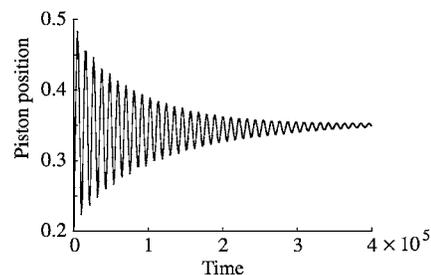

FIG. 1. Piston position versus time, obtained from MD simulations. Piston mass is $M = 512$ where particle mass, m, is taken as unity; other parameters are as in Fig. 5.
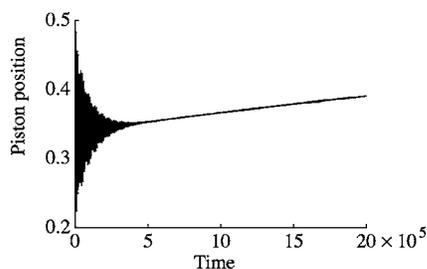
016121-1

FIG. 2. Same as Fig. 1, but extended fivefold in time.

FIG. 4. Piston position, normalized by L_x, versus time for increasing values of M. The other parameters are $L_x=4800$, $n=0.002\,778$, with $M/L_y=4/3$, $X_p(0)=L_x/5$ and $v_p(0)=0$.

Our interest in this paper is mainly with respect to this last issue. We first reiterate that the above-mentioned paradox is directly related to the order in which the limits are taken, so that it has to be put on a purely mathematical ground. Here we focus only on actual physical systems where the system size, although arbitrarily large, remains nevertheless finite. But even in this case the problem is not solved completely. In fact, it is clear that in the limit of a large piston mass, the much slower Brownian motor regime is practically eliminated. But then the resulting degeneracy of the mechanical equilibrium state raises the question as to whether it can be predicted from the initial state by a macroscopic theory.

In contrast to most previous theoretical approaches based on kinetic theory (e.g., [4,14–17]), we investigate this question by means of standard hydrodynamics. A further distinction is that practically all the earlier numerical studies were based on point particle (collisionless) gases [5,6] while here we use full molecular dynamics (MD) simulations of hard disk fluids [7,18]. A detailed comparison of these microscopic simulations with hydrodynamics predictions will be presented in the next section. The results are used as a guideline to build a simple macroscopic theory with progressively increasing levels of sophistication (Secs. III and IV), leading finally to a closed piston equation of motion [18] (Sec. V). We will then show that this equation describes very accurately the motion of a heavy piston from an arbitrary initial state up to the final mechanical equilibrium state. This in turn allows us to express the limitations of the theory's validity and the main characteristics of the piston dynamics, such as the period of oscillations, the relaxation time, and so forth, in terms of the basic parameters of the system (Sec. VI). Finally, a summary of the work, with its advantages and weaknesses, will be presented in Sec. VII where some perspectives for future work are also discussed.

II. MOLECULAR DYNAMICS VERSUS HYDRODYNAMICS

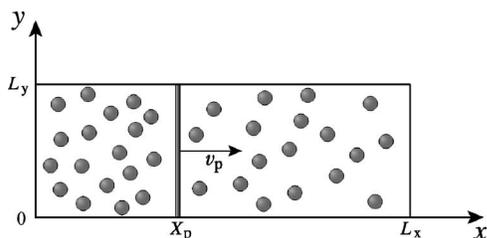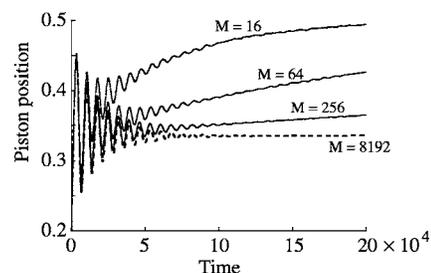We consider a two-dimensional fluid composed of N hard disks of diameter d and mass m. The disks are separated in

FIG. 3. Hard disk molecular dynamic setup.

two groups of $N/2$ particles each, left (L) and right (R) of the piston. They are enclosed in a rectangular box of surface $S=L_x\times L_y$ ($L_x\gg L_y$) oriented along the x and y axes (see Fig. 3). To simplify the discussion, lengths and masses will be scaled by the disk diameter d and mass m, respectively, i.e., $d=m=1$. Similarly, by an appropriate scaling of time and energy, the equilibrium temperature and the Boltzmann's constant are set to unity. Initially, the piston is at rest, located at position $X_p(0)=L_x/5$, and both compartments are in equilibrium with same temperature $T_L(t=0)=T_R(t=0)=T_0=1$ (in system units). Note that due to this asymmetric initial position, the initial pressures left and right are not equal.

We have performed extensive MD simulations for different values of the main parameters (piston mass M, system width L_y, total number of hard disks N, etc). The system length and the number density are fixed to $L_x=4800$ and $n=1/360\approx0.002\,778$. Note that for such a low number density the fluid behaves basically as a Boltzmann gas. An ensemble average over different realizations (i.e., different simulation runs) leads to the "macroscopic" quantities of interest, namely the fluid state variables, as well as the piston position $X_p(t)$ and velocity $v_p(t)$. These results are then compared with the corresponding hydrodynamic predictions. In this section the ratio of piston mass to system width is always $M/L_y=4/3$, with a piston mass ranging from $M=16$ ($L_y=12$, $N=160$) to $M=8192$ ($L_y=6144$, $N=81\,920$).

For the chosen set of parameters, a detailed numerical analysis shows that the separation between the short- and long-time regimes, corresponding respectively to the relaxation to the "mechanical" and "full thermodynamic" equilibrium states, becomes apparent for a piston mass of about $M\approx256$. This is illustrated in Fig. 4 where the piston position versus time is shown for increasing values of M. As can be seen, for $M=16$ there is no separation between short- and long-time regimes; the piston oscillates and smoothly relaxes to the final thermodynamic equilibrium state ($X_p/L_x=0.5$). Increasing the mass by a factor of four ($M=64$) does not change the situation much, except that the relaxation time is now significantly larger. Another fourfold increase (to $M=256$) is required before the expected time separation regimes become apparent. The last curve (dashed line) corresponds to $M=8192$, which well approximates the behavior of the system in the thermodynamic limit ($M\to\infty$, $L_y\to\infty$, $N\to\infty$ with $M/L_y=4/3$ and $N/L_xL_y=n\approx0.002\,778$). In this case the piston undergoes a damped oscillatory motion and quite rapidly reaches the "mechanical" equilibrium state. Its

trajectory then remains perfectly flat (to within the statistical errors) for the rest of time presented in the figure. Of course this behavior lasts only for a finite period of time, typically of the order of the time scale shown in the figure ($t \approx 2 \times 10^5$). In general, no matter how massive the piston, there always exists a sufficiently long time scale after which the system will eventually reach its full thermodynamic equilibrium state. As we already pointed out in the Introduction, the intermediate mechanical equilibrium state can be considered as the genuine final equilibrium state of the system only in the thermodynamic limit, provided that this limit is taken prior to the limit $t \to \infty$. Note that for sufficiently large mass ($M > 256$), the first stage of the piston's motion becomes practically independent of its mass, mainly because the ratio M/L_y is kept constant. Other cases will be considered in the next section.

The (left and right) hydrodynamic equations, corresponding to the above microscopic setup, read [19]

$$\frac{\partial \rho}{\partial t} = -\nabla \cdot (\rho \mathbf{v}), \tag{1}$$

$$\rho \frac{\partial \mathbf{v}}{\partial t} = -\rho(\mathbf{v} \cdot \nabla)\mathbf{v} - \nabla P - \nabla \cdot \boldsymbol{\sigma}, \tag{2}$$

$$\rho c_v \frac{\partial T}{\partial t} = -\rho c_v \mathbf{v} \cdot \nabla T - T\left(\frac{\partial P}{\partial T}\right)_\rho \nabla \cdot \mathbf{v} + \nabla \cdot (\kappa \nabla T) - \sigma_{i,j} \frac{\partial v_i}{\partial x_j}, \tag{3}$$

where ρ is the mass density, P is the hydrostatic pressure, c_v is the constant-volume specific heat, and $\boldsymbol{\sigma}$ is the two-dimensional stress tensor:

$$\sigma_{i,j} = -\eta\left(\frac{\partial v_i}{\partial x_j} + \frac{\partial v_j}{\partial x_i} - \delta_{i,j} \nabla \cdot \mathbf{v}\right) - \zeta \delta_{i,j} \nabla \cdot \mathbf{v}, \tag{4}$$

where η and ζ are the shear and bulk viscosities, respectively. The boundary conditions are those of thermally isolated stress-free rigid walls in the x direction (direction of the piston motion) and periodic in the y direction. In particular,

$$v_x(x = X_p) = v_p, \quad v_x(x = 0) = v_x(x = L_x) = 0,$$

$$\left.\frac{\partial T}{\partial x}\right|_{x=X_p} = \left.\frac{\partial T}{\partial x}\right|_{x=0,L_x} = 0. \tag{5}$$

Note that the particle flux, and thus the associated linear momentum and energy fluxes, must vanish at the fluid-piston boundaries.

To solve the hydrodynamic equations, we still need the equation of state and the explicit form of transport coefficients. As is well known, for hard disks fluids the equation of state is is well approximated by [20]

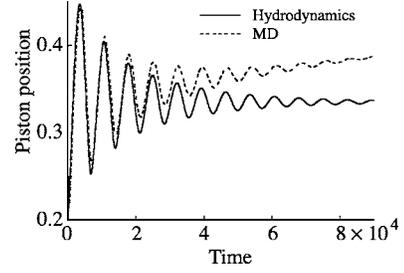$$P = nk_B T \phi(n) \tag{6}$$

with

FIG. 5. Piston position, normalized by L_x, versus time for $M = 64$. The other parameters are $L_x = 4800$, $L_y = 48$, $n = 0.002\,778$, $X_p(0) = L_x/5$ and $v_p(0) = 0$.

$$\phi(n) = \frac{1 + \pi^2 n^2/128}{(1 - \pi n/4)^2}, \tag{7}$$

where n is the number density (recall that the disk diameter d is set to unity in system units). Note that the results presented in this article are for a dilute gas ($n = 1/360$) for which $\phi \approx 1$. As for the transport coefficients, we rely on their Enskog expressions [20]:

$$\eta = 0.2555 n\sqrt{\pi m k_B}\left(1 + \frac{2}{\pi n g_2} + 0.4365 \pi n g_2\right)\sqrt{T}, \tag{8}$$

$$\zeta = 0.1592 \pi^{3/2} n^2 g_2 \sqrt{T}, \tag{9}$$

$$\kappa = 1.029 n k_B^{3/2} \sqrt{\pi/m}\left(\frac{3}{2} + \frac{2}{\pi n g_2} + 0.4359 \pi n g_2\right)\sqrt{T}, \tag{10}$$

where g_2 is the pair correlation function at contact:

$$g_2 = \frac{1 - 7n\pi/64}{(1 - n\pi/4)^2}. \tag{11}$$

Finally, Newton's equation of motion for the piston reads

$$M\frac{d^2 X_p}{dt^2} = L_y(P_L^{xx} - P_R^{xx})_{x=X_p}, \tag{12}$$

where $P^{xx} = P - (\eta + \zeta)\partial v_x/\partial x$ is the pressure tensor, contracted in the x direction. We note that the hydrodynamic equations, and thus the piston equation of motion, are uniquely specified without any adjustable parameter. We now compare the numerical solution of these equations with the result obtained through the corresponding MD simulation.

We first consider a relatively small piston mass $M = 64$ (with $L_y = 48$). Figure 5 shows the (ensemble) average piston position versus time. For this relatively small mass there is no clear separation between the short- and long-time regimes (cf. Fig. 4). Nevertheless, hydrodynamics and MD are in quantitative agreement for the first two or three oscillations, with deviations increasing at longer times. The same behavior is observed for the average temperatures and densities on each side of the piston (see Fig. 6).

The situation is somehow different for the piston velocity, where very good quantitative agreement between MD and hydrodynamics is observed for a span of many oscillations
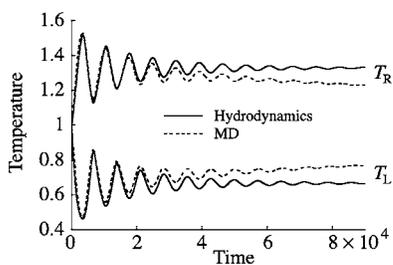
FIG. 6. Left and right temperature profiles versus time. Parameters are as in Fig. 5.

(cf. Fig. 7). This result, at first unexpected, is related to the fact that the degeneracy of states, which occurs at the thermodynamic limit, concerns mainly the final piston position but not its final velocity, which is simply zero. For finite piston mass, the piston velocity does not vanish at the intermediate quasi-equilibrium state; it nevertheless becomes extremely small so that the actual discrepancy with MD remains within the estimated statistical errors (about 1%). What is perhaps more striking is the behavior of the average fluid pressure. As can be seen in Fig. 8, surprisingly good quantitative agreement is found even for a piston mass as small as $M=1$ ($L_y=48$, $N=640$). So far, we have no convincing argument to explain this observation.

As we have shown above, for the set of parameters that we have adopted, the separation between the short- and long-time regimes becomes apparent for larger piston mass starting at about $M \approx 256$. As a consequence, the agreement between hydrodynamics and MD improves dramatically as soon as $M > 256$. This is illustrated in Fig. 9 where quantitative agreement is demonstrated for a piston mass $M=512$. For instance, the discrepancy remains below 3%, long after the mechanical equilibrium state has been reached ($t=1.5 \times 10^5$), and drops below the estimated statistical errors (about 1%) for $M=1024$. These observations lead us to the first major conclusion of this work. While hydrodynamics cannot describe the details of the very long time scale regime, dominated by the fluctuation-driven heat transfer by the piston's Brownian motion, it quite accurately predicts the damped oscillatory motion leading to the mechanical equilibrium state. This in turn suggests that a simple macroscopic theoretical description must be possible in the limit of a large piston mass. We now set up such a description at progressively increasing levels of sophistication.

III. A SIMPLE HYDRODYNAMIC THEORY

The equation (12) shows that the motion of the piston is expected to be notably slow in the limit of large ratio M/L_y,
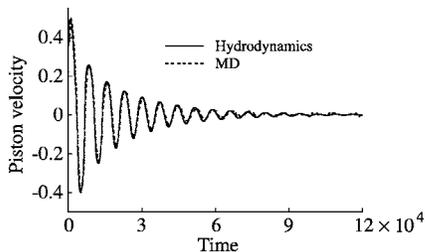

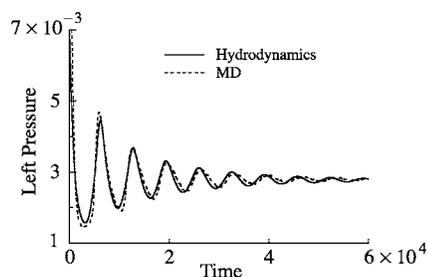FIG. 7. Piston velocity versus time. Parameters are as in Fig. 5.

FIG. 8. Left pressure profile for $M=1$. The other parameters are as in Fig. 5.

in which case one can reasonably assume that each compartment undergoes an (quasi-static) adiabatic transformation. For the case of a dilute gas, this implies that $PV^\gamma = P_0 V_0^\gamma$ =const, where γ is the ratio of the constant-pressure and constant-volume specific heats, c_p/c_v, and the subscript "0" refers to initial values at $t=0$. On the other hand, $V_L(t) = X_p(t)L_y$ and $V_R(t) = [L_x - X_p(t)]L_y$, where the subscripts "L" and "R" refer to the left and right compartments, respectively. Neglecting all possible dissipative processes, the Newtonian equation of motion for the piston reads

$$M\frac{d^2 X_p}{dt^2} = L_y(P_L - P_R) = L_y^{1-\gamma}\left(\frac{C_L}{X_p^\gamma} - \frac{C_R}{(L_x - X_p)^\gamma}\right), \quad (13)$$

where the C (left and right) is a constant given by $C = P_0 V_0^\gamma$. This is a closed piston equation of motion that has been already obtained on the basis of dynamical systems theory [14]. Simple kinetic theory, based on Maxwellian point-particle (i.e., collisionless) gases, leads basically to the same result [15–17]. For the case of a dilute two-dimensional gas under consideration here, we have $\gamma=2$ and $P_0 V_0 = Nk_B T_0/2$ so that

$$M\frac{d^2 X_p}{dt^2} = mN\frac{v_{th}^2}{2}\left(\frac{X_p(0)}{X_p^2} - \frac{L_x - X_p(0)}{(L_x - X_p)^2}\right), \quad (14)$$

where $v_{th} = (k_B T_0/m)^{1/2}$ is the thermal velocity (equal to 1 in system units). It has been shown recently that the solution of (14) is in poor agreement with MD simulations [18]. Our main purpose in this article is to set up an improved theory, based on hydrodynamics, that includes the effect of dissipative processes as well.

In deriving the result (13), we have implicitly assumed that the left and right pressure difference accelerates only the piston and not the embedded fluid. This in turn implies that
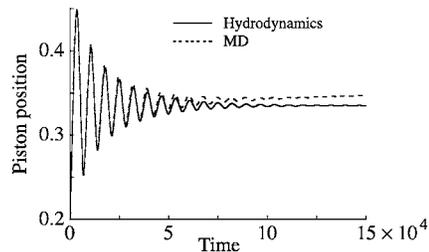

FIG. 9. Piston position, normalized by L_x, versus time for $M=512$. The other parameters are as in Fig. 4.

the fluid velocity remains identically zero in the course of time, if initially so. However, the velocity of the fluid layer in direct contact with the piston is obviously equal to the velocity of the piston, while remaining zero for the fluid layers at the opposite, outer boundaries. Hence, instead of assuming zero fluid velocity throughout the system, a less restrictive assumption is to consider a linear fluid velocity profile along the x direction:

$$v_L(x,t) = v_p(t)\frac{x}{X_p(t)}, \quad v_R(x,t) = v_p(t)\frac{L_x - x}{L_x - X_p(t)}, \quad (15)$$

where v_L and v_R represent the x component of the fluid velocity in the left and right compartments, respectively, and $v_p = dX_p/dt$ is the piston velocity. The y component of the fluid velocity is not affected by the piston's motion so that it remains zero if initially so. This in turn implies that the hydrodynamical variables remain functions of one spatial coordinate only (coordinate x). To obtain the appropriate piston equation of motion we now solve the hydrodynamic equations, it being understood that the assumption (15) replaces the momentum equation (2).

Inserting (15) into the continuity equation (1), we first prove (see Appendix A) that the density remains homogeneous, if initially so, its explicit expression being given by

$$\rho_L(t) = \frac{mN}{2L_y X_p}, \quad \rho_R(t) = \frac{mN}{2L_y(L_x - X_p)}. \quad (16)$$

Using this result and the energy conservation principle, we next derive (see Appendix B) the general form of the piston equation of motion:

$$\hat{M}\frac{d^2 X_p}{dt^2} = L_y(\bar{P}_L - \bar{P}_R) - L_y v_p\left(\frac{\bar{\Gamma}_L}{X_p} + \frac{\bar{\Gamma}_R}{(L_x - X_p)}\right), \quad (17)$$

where $\bar{P}$ and $\bar{\Gamma}$ are the spatially averaged hydrostatic pressure P and viscosity coefficient $\Gamma = \zeta + \eta$, respectively, and

$$\hat{M} = M\left(1 + \frac{mN}{3M}\right) \quad (18)$$

is a "renormalized" piston mass. As mentioned above, in this paper we restrict ourselves to the case of hard disk fluids for which the hydrostatic pressure is a linear function of the temperature [cf. Eq. (6)]. As a result, $\bar{P}(\rho, T) = P(\rho, \bar{T})$ and the space-averaged temperature $\bar{T}$ is precisely the "homogeneous" temperature that we used in the simple adiabatic theory (13).

However, unless we neglect the dissipative processes, the equation of motion (17) remains coupled to the temperature equation (3), since we do not yet have an explicit form of $\bar{T}$ in terms of piston position and velocity. To solve this problem, we need an additional assumption regarding the viscosity coefficient Γ. In general, transport coefficients are taken to be constant since their dependence on state variables is weak (e.g., for a Boltzmann gas $\Gamma \propto \sqrt{T}$). Numerical solution of the hydrodynamic equations (1)–(3) fully support this approximation, the discrepancies remaining always below 3%.
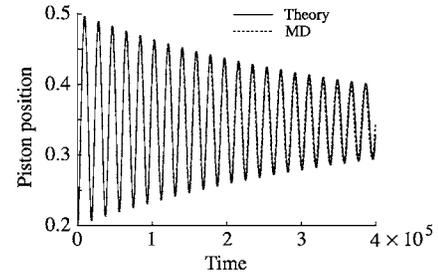

FIG. 10. Piston position obtained from MD and the numerical solution of Eqs. (17) and (19), for $M=2048$. The other parameters are $N=640$, $L_x=4800$, $L_y=48$, $X_p(0)=L_x/5$, and $v_p(0)=0$.

However, for the sake of generality, here we shall adopt the less restrictive assumption that the viscosity coefficient depends only on the "global" space averaged state variables, i.e., $\Gamma = \Gamma(\rho, \bar{T})$. Within this rather weak assumption, we prove in Appendix C that, as with density, the temperature remains homogeneous over time, if initially so, and obeys [cf. Eq. (C9) in Appendix C]

$$\frac{\partial T_L}{\partial t} = -\frac{v_p}{X_p}\phi_L T_L + \frac{2L_y}{k_B N}\frac{\Gamma_L}{X_p}v_p^2 \quad (19)$$

with a similar expression for the right compartment. Note that the function $\phi(n) = \phi(n(X_p))$ is defined in (7) and $\Gamma_L \equiv \Gamma(\rho_L, T_L)$, where we have dropped the "bar" notation since temperature remains homogeneous.

The hydrodynamic problem is now reduced to a set of three coupled ordinary differential equations: the piston equation of motion (17) and the (left, right) temperature equations (19). To check the validity of this simplified theory, we consider a whole new set of MD simulations with $L_y=48$, $N=640$ hard disks, $L_x=4800$ (as before $n=0.002\,778$), and a piston mass ranging from $M=64$ to $M=8192$. Unlike the MD simulations presented in Sec. II, here the system width L_y and the number of particles N are fixed, so that the piston motion gradually slows down as we consider increasing values of M, allowing comparison with the theory. Note that the relatively small number of particles ($N=640$) allows one to consider a large number of sample paths (typically of the order of 10^5) within reasonable computational time, lowering significantly the statistical error.

As seen in Fig. 10, where the piston position versus time is shown, excellent agreement is observed between MD and the corresponding numerical solution of Eqs. (17) and (19), even for the relatively moderate piston mass of $M=2048$. Specifically, the observed amplitude discrepancy remains below 1% after 15 periods of oscillations, with a corresponding phase shift discrepancy of about 0.3%. Unfortunately, an analytical treatment appears to be extremely difficult without further simplifications. This issue will be addressed in the next section.

IV. THE IDEAL GAS LIMIT

Consider the temperature equation (19). To obtain a closed piston equation of motion, one has to express the (left

and right) temperature in terms of piston position and velocity. This, however, proves to be extremely difficult mainly because of the (nonlinear) state dependence of the viscosity coefficient that appears in the viscous heating term [the formal solution is given in Appendix C, Eq. (C10)]. On the other hand, in the limit of large piston mass, the piston velocity becomes quite small (recall that the system width and the number of particles are fixed). The viscous heating term can thus be neglected since it is proportional to the square of the velocity gradient. This approximation is further justified in view of the fact that the viscous heating term is also inversely proportional to the total number of particles N, which is usually quite large. Within this restriction, one can easily show that (cf. Appendix C):

$$T(t) = T_0 e^{-\Phi(t)} \tag{20}$$

with

$$\Phi(t) = \int_{X_p(0)}^{X_p(t)} \frac{\hat{\phi}(\zeta)}{\zeta} d\zeta, \tag{21}$$

where the function $\phi(n) = \phi(n(X_p)) = \hat{\phi}(X_p)$ is defined in (7) and the subscript "0" refers to initial values at $t=0$. The equation of state (6) then implies

$$P(t) = P_0 \frac{X_p(0)}{X_p(t)} \frac{\hat{\phi}}{\hat{\phi}_0} e^{-\Phi(t)}. \tag{22}$$

Inserting (20) and (22) into (17) leads to a closed piston equation of motion.

For a dilute two-dimensional gas, as considered here, $\phi \approx 1$ so

$$\Phi(t) = \ln \frac{X_p(t)}{X_p(0)}. \tag{23}$$

The temperature (20) and pressure (22) thus read

$$T(t) = T_0 \frac{X_p(0)}{X_p(t)}, \quad P(t) = P_0 \left(\frac{X_p(0)}{X_p(t)} \right)^2 \tag{24}$$

so that

$$X_p(t)T(t) = \text{const}, \quad X_p^2(t)P(t) = \text{const}. \tag{25}$$

Since $\gamma = 2$, this latter result implies that $PV^\gamma = \text{const}$. We thus arrive at the conclusion that the system (piston+gas) undergoes an adiabatic transformation despite the presence of dissipative damping terms appearing in the pressure tensor [cf. Eq. (17)]. It should however be realized that this property is a direct consequence of neglecting the viscous heating term in the temperature equation [cf. Eq. (C10) in Appendix C].

It is instructive to analyze first the case of an idealized system, ignoring dissipative processes. In this case, the equation (17) becomes identical to the equation (14) obtained from the simple adiabatic theory, but with the replacement of the piston mass M by $\hat{M} = M + mN/3$. The fact that the pressure difference across the piston also induces an acceleration of the fluid thus results in a mere renormalization of the piston mass. While this correction becomes vanishingly small in the limit of large M, it gives a dramatic improve-
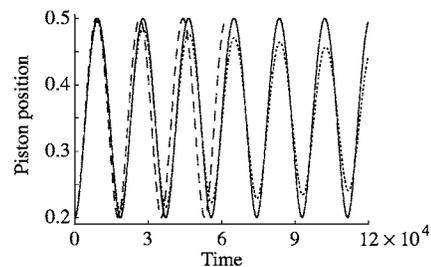

FIG. 11. Piston position versus time for $M=2048$. The dotted line represents MD results, the dashed line the simple adiabatic theory, Eq. (14), and the full line the improved adiabatic theory predictions. The other parameters are as in Fig. 10.

ment over the simple theory, Eq. (14), for moderate values of M. This is illustrated in Fig. 11 where the piston position versus time for $M=2048$ is shown. Clearly the profile based on the simple adiabatic theory becomes significantly out of phase with respect to MD results after only two oscillations. This is not the case for the improved adiabatic theory where perfectly synchronized oscillations are observed even after seven oscillations.

The relevance of the improved theory is further highlighted by computing explicitly the piston's period of oscillation. Upon introducing dimensionless variables $x_p(t) = X_p(t)/L_X$, $x_0 = X_p(0)/L_X$, and

$$\tau = t \frac{v_{th}}{\sqrt{2}L_x} \left(\frac{mN}{\hat{M}} \right)^{1/2}, \tag{26}$$

Eq. (17) becomes [recall that $v_{th} = (k_B T_0/m)^{1/2}$ is the thermal velocity]

$$\frac{d^2 x_p}{d\tau^2} = \frac{x_0}{x_p^2} - \frac{1-x_0}{(1-x_p)^2} \tag{27}$$

subject to initial conditions $x_p = x_0$ and $dx_p/d\tau = 0$ at $\tau = 0$. This equation is identical to the Newton equation for a particle (the piston) of unit mass in a force field, derived from the potential

$$U(x_p) = \frac{x_0}{x_p} + \frac{1-x_0}{1-x_p}. \tag{28}$$

Conservation of total energy implies

$$\frac{1}{2} \left(\frac{dx_p}{d\tau} \right)^2 + U(x_p) = U(x_0) = 2. \tag{29}$$

The exact time-dependent solution of (27) can be found by integration of the energy equation (29) in terms of elliptic functions. In particular, the (scaled) period τ_p of the piston oscillations, for $x_0 = \frac{1}{5}$, reads

$$\tau_p = \sqrt{2} \int_{x_0}^{1/2} \frac{dx}{\sqrt{U(x_0) - U(x)}} \approx 1.456. \tag{30}$$

Figure 12 clearly shows that the estimated period of oscillations, obtained from MD simulations, approaches quite rapidly the corresponding theoretical value as the piston mass increases. For instance, the discrepancy is about 0.7% for
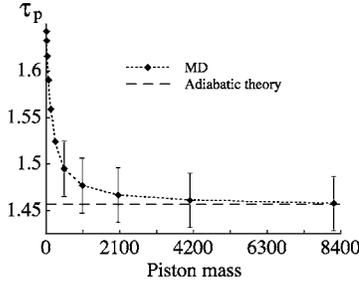
FIG. 12. The estimated (scaled) period of oscillations of the piston versus M for $x_0 = \frac{1}{5}$. The statistical errors are about 2%. The dashed straight line represents the corresponding adiabatic approximation, Eq. (30). The other parameters are as in Fig. 10.

$M = 2048$, far below the estimated statistical errors (about 2%). Note that Eq. (14), based on the simple adiabatic theory, leads to a discrepancy of about 6%, which is nearly ten times worse than the improved adiabatic theory.

Furthermore, we observe that the "kinetic energy" in (29) vanishes at $x_p = x_0$, as required by the initial condition, but also at $x_p = \frac{1}{2}$, implying that the extreme position reached by the piston, in an ideal system, is the middle of the system. Now, since the principal effect of viscous dissipation is to slow the piston's motion, we arrive at the conclusion that the piston will never cross the middle of system, independently of the parameter values and of its initial position. This somehow unexpected prediction is nicely confirmed by MD simulation results presented in Fig. 13.

Finally, even though the above improved adiabatic theory does not include dissipation, one expects that the "final" position of mechanical equilibrium, x_{eq}, will correspond to the minimum of $U(x)$, namely

$$x_{eq} = \frac{x_0 - \sqrt{x_0(1-x_0)}}{2x_0 - 1}. \qquad (31)$$

Again this is (for large mass) in perfect agreement with MD. For example, for $x_0 = \frac{1}{5}$ and $M = 2048$, the estimated (mechanical) equilibrium position from MD is 0.34±.02, while the result (31) predicts $x_{eq} = \frac{1}{3}$.

V. INCLUDING DISSIPATION

In a dilute gas, the bulk viscosity coefficient $\zeta \approx 0$ and the shear viscosity coefficient η is independent of the density, but depends on temperature as [cf. Eq. (8)]:
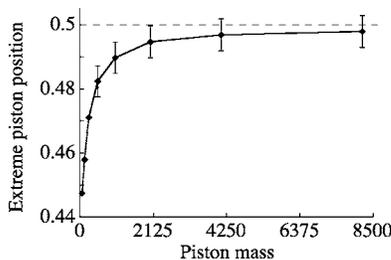

FIG. 13. The piston first extreme position versus M for $x_0 = \frac{1}{5}$. Estimated statistical errors are about 1%. The other parameters are as in Fig. 10.

$$\eta = \eta_0 \sqrt{T}, \quad \eta_0 \approx \frac{1}{2d} \sqrt{\frac{mk_B}{\pi}}. \qquad (32)$$

Inserting this result into (17) and using relations (24), one finds the following dimensionless closed piston equation of motion:

$$\frac{d^2 x_p}{d\tau^2} = \frac{x_0}{x_p^2} - \frac{1-x_0}{(1-x_p)^2} - \mu \frac{dx_p}{d\tau} \left(\frac{x_0^{1/2}}{x_p^{3/2}} + \frac{(1-x_0)^{1/2}}{(1-x_p)^{3/2}} \right), \qquad (33)$$

where

$$\mu = \eta_0 L_y \left(\frac{2}{\hat{M} N k_B} \right)^{1/2} \approx \frac{L_y}{2d} \left(\frac{2m}{\pi \hat{M} N} \right)^{1/2} \qquad (34)$$

is a dimensionless friction coefficient. For $M = 2048$, the numerical solution of this equation has an amplitude discrepancy, compared with MD simulation results, of about 6% after 15 periods of oscillation (recall that it was below 1% for the general theory presented in Sec. III, Fig. 10). The discrepancy, however, drops to about 2% for $M = 4096$ and to less than 1% for $M = 8192$. We thus conclude that, for sufficiently large piston mass, Eq. (33) describes correctly the piston motion from an arbitrary initial position x_0 to the corresponding mechanical equilibrium rest position x_{eq}, given by (31).

Unfortunately, an analytical treatment of Eq. (33) appears to be quite difficult in view of the highly nonlinear character of the viscous damping term. Further simplifications can be achieved provided we restrict ourselves to initial piston positions x_0 close to the thermodynamic equilibrium position of $\frac{1}{2}$. Recalling that $x_0 < x_{eq} \leqslant \frac{1}{2}$ [cf. Eq. (31)], one may linearize x_p around x_{eq} in Eq. (33), obtaining the following damped harmonic oscillator equation of motion (see also Ref. [13]):

$$\frac{d^2 x_p}{d\tau^2} + 2\beta \frac{dx_p}{d\tau} + \omega_0^2 (x_p - x_{eq}) = 0 \qquad (35)$$

with

$$\beta = \frac{\mu}{2} \left(\frac{x_0^{1/2}}{x_{eq}^{3/2}} + \frac{(1-x_0)^{1/2}}{(1-x_{eq})^{3/2}} \right) = 2\mu + O((x_0 - 1/2)^2) \quad (36)$$

and

$$\omega_0^2 = \frac{2x_0}{x_{eq}^3 (1-x_{eq})} = 16 + O((x_0 - 1/2)^4). \qquad (37)$$

The solution of (35) reads

$$x_p(\tau) = A \exp(-\beta\tau)\cos(\omega\tau + \phi), \qquad (38)$$

where $\omega = (\omega_0^2 - \beta^2)^{1/2}$ is the angular frequency, $A = (x_0 - x_{eq})/\cos(\phi)$, and $\tan(\phi) = -\beta/\omega$. The period τ_h of oscillations is thus given by

$$\tau_h = \frac{2\pi}{(\omega_0^2 - \beta^2)^{1/2}} \approx \frac{2\pi}{\omega_0} \approx \frac{\pi}{2}. \qquad (39)$$

To check the validity of (35), we consider another set of microscopic simulations, with the same parameter values as before, except that the initial piston position is now set to $x_0 = 2/5$ (instead of 1/5). In Fig. 14 we compare the density
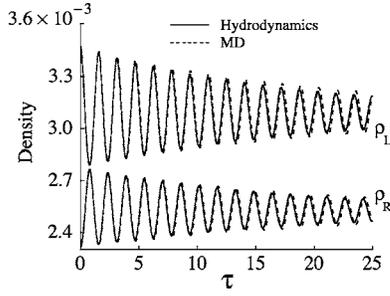
FIG. 14. The left and right density profiles versus (scaled) time, for $M=1024$ and $x_0=2/5$. The other parameters are as in Fig. 10.
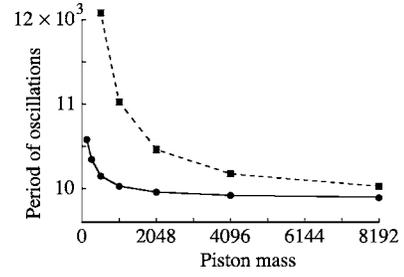

FIG. 15. The piston period of oscillations versus mass, scaled either by $(M/mN)^{1/2}$ (dashed line) or by $(\hat{M}/mN)^{1/2}$ (solid line), for an initial piston position $x_0=\frac{1}{5}$. The other parameters are as in Fig. 10.

as a function of time, as obtained from MD, with its corresponding harmonic approximation, based on (38). Surprisingly, a quite good quantitative agreement is observed already for $M=1024$ where the period of oscillations, estimated from MD simulations, is about 1.556 ± 0.030, whereas (39) gives 1.57, a discrepancy of less than 1.5%. However, this discrepancy does not improve for larger piston mass. Detailed numerical analysis shows that the validity of the harmonic approximation is basically controlled by the proximity of the initial piston position to the thermodynamic equilibrium position (middle of the system), provided $M \geqslant 512$. Nevertheless, this approximation proves to be quite useful in providing explicit expressions for the main characteristics of the piston dynamics.

VI. VALIDITY OF THE SIMPLE THEORY

The greater the mass of the piston, the slower its motion. From this intuitive observation, we derived a simple theory that accurately describes the dynamics of the system, provided that the piston mass is sufficiently large. Yet so far we have not specified what is meant by the criterion of a "sufficiently large" piston mass. Large compared to what? How do the other parameters of the system, such as the system dimension $L_x \times L_y$ or the fluid mass mN, influence the validity of the theory? To answer these questions, we need to determine the characteristics of the piston's dynamics, such as the period of oscillations, the relaxation time, and so forth, in terms of the basic parameters of the system.

We first consider the period of oscillations and notice that its value, obtained in MD simulations, varies only from 1.45 to 1.60 (in dimensionless units) for a broad range of piston mass ($64 \leqslant M \leqslant 8192$) and for widely separated initial positions ($x_0=0.2$ or $x_0=0.4$). The harmonic value $\tau_h=\pi/2 \approx 1.57$ thus provides a relatively good estimate of the oscillation period. Switching back to the original time variable (i.e., $\tau \rightarrow t$), the piston's period of oscillations is [cf. Eq. (26)]:

$$t_p = \frac{\pi\sqrt{2}}{2v_{th}}L_x\left(\frac{\hat{M}}{mN}\right)^{1/2}. \tag{40}$$

Recall that $v_{th}=(k_BT_0/m)^{1/2}$ is the thermal velocity (equal to 1 in system units).

Interestingly, for fixed N and L_x the period scales as the square root of the renormalized piston mass, $(M+mN/3)^{1/2}$,

and not as $M^{1/2}$. For sufficiently large piston mass, as compared to the fluid mass, these scalings are equivalent, but when the two masses are of the same order of magnitude we have the opportunity to determine whether the renormalization of the piston mass is a spurious artifact of the linear fluid velocity assumption, or if it has a fundamental, physical origin. Detailed MD simulations clearly indicate the latter. This is shown in Fig. 15 where the period of oscillations, scaled either by $(M/mN)^{1/2}$ or by $(\hat{M}/mN)^{1/2}$, versus M, is depicted for $x_0=0.2$. As can be seen, both sets converge to a constant value, as the piston mass is increased, but the latter converges much faster than the former. Furthermore, for large M ($M>2048$), the measured value of the period is about 9904, whereas the harmonic approximation (40) gives 10 663, a discrepancy close to 7%. This result clearly confirms the validity of (40) since the MD simulations were done for an initial piston position of $x_0=0.2$, for which the harmonic approximation is not accurate.

The situation is quite similar for the relaxation time β^{-1} [cf. Eq. (36)] where, upon switching back to the original time variable, one gets

$$t_{relax} = C\frac{\sqrt{\pi}}{v_{th}}L_x\left(\frac{\hat{M}d}{mL_y}\right). \tag{41}$$

The numerical constant C depends weakly on the initial piston position x_0 and it is practically independent of M. For instance, $C(x_0=0.4) \approx 0.50$ whereas $C(x_0=0.2) \approx 0.51$. Note that (41) implies that if the ratio M/L_y is constant, then the relaxation time is nearly independent of the piston's mass. As shown in Sec. II, this prediction is nicely confirmed by MD simulations for $M>256$ [cf. Fig. 4]. Note that a similar relaxation time was predicted by Crosignani and Di Porto [13] for a piston embedded in a point-particle (collisionless) fluid maintained in a Maxwellian thermal equilibrium state.

Another interesting quantity is the maximum piston speed, which is reached at about the first quarter period of oscillation, after the piston is released. The corresponding piston position is the mechanical equilibrium position x_{eq}. Neglecting viscous dissipation, relation (29) gives (in the original space and time variables)

$$|v_p|_{max} = v_{th}\sqrt{2-U(x_{eq})}\left(\frac{mN}{\hat{M}}\right)^{1/2}. \tag{42}$$

This implies that, in ideal systems, the maximum speed of a massive piston is proportional to the square root of the ratio
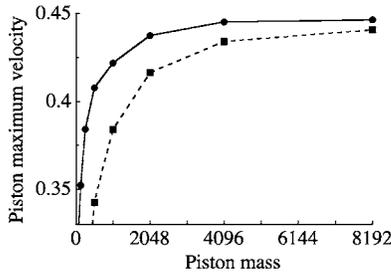
FIG. 16. The piston maximum speed $|v_p|_{max}$ versus mass, scaled either by $(mN/M)^{1/2}$ (dashed line) or by $(mN/\hat{M})^{1/2}$ (solid line), for an initial piston position $x_0=\frac{1}{5}$. The other parameters are as in Fig. 10.

of the fluid mass and the (renormalized) piston mass, the proportionality factor being only a function of the piston's initial position x_0 [cf. Eq. (31)]. Detailed MD simulations confirm this conclusion as shown in Fig. 16 where the maximum piston speed, scaled either by $(mN/M)^{1/2}$ or by $(mN/\hat{M})^{1/2}$, versus M, is presented for $x_0=0.2$. As the piston mass is increased both sets of data converge to a constant value but here again the rate of convergence of the latter data set, using the renormalized mass $\hat{M}$, is much faster than for the set scaled by M. Furthermore, the measured maximum piston speed for the largest piston mass ($M=8192$) is about 0.446, as compared with the ideal system approximation (42) prediction of 0.447.

There is a simple explanation for this remarkable agreement: The MD simulations, presented in Fig. 16, were performed for fixed system width ($L_y=48$). In this scenario the relaxation time increases linearly with piston mass [cf. Eq. (41)], diminishing significantly the effect of viscous damping on the early stage dynamics (e.g., $t < t_p$). Therefore, in this initial stage, the system behaves essentially as if it were an ideal system, for which (42) is exact. For this very same reason, the discrepancy with the theory increases with L_y, reaching a value of about 7% when the relaxation time becomes comparable to the period of oscillations. Nevertheless, since the principal effect of viscous dissipation is to slow the piston's motion, its maximum velocity is bounded by the corresponding ideal system limit, given by Eq. (42). The general result is thus obtained upon replacing the equality sign in Eq. (42) by a bounding inequality sign (i.e., by "$\leq$"). Note that in all cases the maximum piston speed remains well below the sound speed, $\sqrt{\gamma k_B T_0/m} = \gamma^{1/2} v_{th}$, so shock waves are not produced by the piston's motion [22].

Relations (40)–(42) completely characterize the piston dynamics. Although their explicit form has been derived directly from the (damped) harmonic approximation, detailed MD simulations show that, for sufficiently large piston mass, they give the correct functional form over a broad range of system parameters, including the piston's initial position x_0 (cf. Figs. 15 and 16). Recalling that, in system units, the thermal velocity, the particles' mass, and their diameter are all set to unity (i.e., $v_{th}=d=m=1$), one may summarize our basic results as

$$t_p \sim L_x \left(\frac{\hat{M}}{M_f} \right)^{1/2}, \qquad (43)$$

$$|v_p|_{max} \sim \left(\frac{\hat{M}}{M_f} \right)^{-1/2}, \qquad (44)$$

$$t_{relax} \sim \frac{L_x}{L_y} \hat{M}, \qquad (45)$$

where $M_f=mN$ is the fluid mass (recall that $\hat{M}=M+mN/3$). For completeness, we also note that the piston cannot cross the thermodynamic equilibrium position (in our case, the middle of the system), regardless of its initial position, provided its initial velocity is zero; this result was proven is Sec. IV (cf. Fig. 13).

The results derived above are quite helpful for understanding the characteristics of the piston dynamics in terms of the main system parameters. But they are not sufficient for establishing the limit of the validity of our simple theory. This issue can be addressed indirectly by the following argument. The theory rests on one major assumption: the linearity of the fluid velocity profile. As we have shown, this assumption, in turn, implies that the state of the fluid remains homogeneous. On the other hand, the piston's motion generates inhomogeneous hydrodynamic modes that propagate through the fluid, eventually damping out by viscous dissipation. For a closed, near equilibrium system of length L, the relaxation times of these inhomogeneous modes are of the order of [21]

$$\tau_k \approx \left(\frac{\Gamma_{eq}}{\rho_{eq}} \frac{k^2 \pi^2}{L^2} \right)^{-1}, \quad k=1,2,\dots . \qquad (46)$$

One can thus expect that the system remains homogeneous if the relaxation time of the slowest ($k=1$) inhomogeneous mode does not exceed the half-period of the piston oscillations, given by Eq. (40). Noticing that near equilibrium the compartment length is about $L_x/2$, the required condition reads

$$\left(\frac{\Gamma_{eq}}{\rho_{eq}} \frac{4\pi^2}{L_x^2} \right)^{-1} < \frac{\pi\sqrt{2}}{4 v_{th}} L_x \left(\frac{\hat{M}}{mN} \right)^{1/2}. \qquad (47)$$

For a dilute Boltzmann gas, $\Gamma \approx \eta$ [cf. Eq. (32)], so that this relation leads to

$$\frac{M}{mN} + \frac{1}{3} > \frac{2}{\pi^5} L_x^2 n_{eq}^2 d^2. \qquad (48)$$

For the MD simulation parameters ($n_{eq}=0.002\,778$, $L_x=4800$, $N=640$, $d=1$), one gets $M > 530$, which is quite close to the result that we obtained in the corresponding microscopic simulation. We thus conclude that this simple argument, based on the separation of time scales for inertial versus viscous processes, yields a good estimate for the limit of validity of our theory.

VII. CONCLUDING REMARKS

In this paper we have analyzed the dynamics of the adiabatic piston using both microscopic molecular dynamics (MD) simulations and the standard hydrodynamic theory. For a sufficiently large piston mass, the dynamics splits in two

well-separated time regimes. Starting from a nonequilibrium configuration (i.e., different pressures in each compartment) the piston performs a damped oscillatory motion reaching, in the first time regime, an intermediate state of "mechanical equilibrium" with the same pressure but different densities and temperatures in each compartment. In the second (much longer) time regime, which is dominated by the fluctuation-driven heat transfer by the piston, a slow relaxation brings the system to the thermodynamic equilibrium state with equal temperatures and densities. While hydrodynamics is unable to describe the piston dynamics in the long time regime, it quite accurately predicts all the details of the first time regime, as demonstrated by the excellent agreement with MD simulations, even for relatively small piston mass (about a third of the fluid mass).

At first sight, the formulation of an equation of motion for a massive piston seems simple. Since the motion of the piston slows down as its mass, M, is increased, it is reasonable to assume that, in the limit of large M, each compartment undergoes an (quasi-static) adiabatic transformation. On the basis of this idea, a macroscopic theory leading to a simple closed piston equation of motion was derived earlier [14,17,18]. This theory, however, neglects completely the motion of the embedded fluid and the associated dissipative processes. Consequently, its predictions are in poor agreement with molecular simulations.

Instead of imposing a zero fluid velocity throughout the system, a less restrictive assumption is to consider a linear fluid velocity profile. With this assumption, and neglecting the spatial dependence of the viscosity coefficient, we have shown that the fluid density and temperature of each compartment remains homogeneous in the course of time, if initially so. The hydrodynamic equations then reduce to a set of three coupled ordinary differential equations that lead to quantitative agreement with MD even when the piston mass is comparable to the fluid mass.

For larger piston mass (about eight times the fluid mass), the viscous heating term in the temperature equation may be neglected. With this approximation, we finally derived a closed piston equation of motion that remains valid from an arbitrary initial state up to the final mechanical rest state. Once more, the validity of this simple equation is fully confirmed through extensive MD simulations. Note that for initial piston positions sufficiently close to the equilibrium state, this equation reduces straightforwardly to a damped harmonic oscillator equation [cf. Eq. (35)].

The main advantage of the (damped) harmonic approximation is that it allows us to express the basic characteristics of the piston dynamics, such as the period of oscillations, the maximum piston velocity, and the relaxation time, in terms of the main system parameters [cf. relations (40)–(42)]. Remarkably, detailed MD simulations show that, for large enough piston mass, these relations feature the correct functional form over a broad range of system parameters, including the piston's initial position x_0, their validity being only limited by the validity of hydrodynamic description [cf. relations (43)–(45)]. One may also recall one last interesting result which concerns the extreme position reached by the piston. As proven in Sec. III, this quantity is bounded by the thermodynamic equilibrium position, i.e., the piston can

never cross the thermodynamic equilibrium position (in our case, the middle of the system), regardless of its initial position, provided its initial velocity is zero.

The success of the theory presented here for the adiabatic piston is yet another confirmation of the robustness of hydrodynamics. As demonstrated by laboratory experiments and molecular simulations [23–25], hydrodynamics remains valid for astronomically large nonequilibrium constraints. Breakdown occurs, however, when the length or time scale of the problem becomes comparable to the molecular (mean free path or time) scale (e.g., [26–28]). Hydrodynamics remains valid since we consider physical scales, for both piston and fluid, that are much larger than the molecular scale. This point raises a related question: What is the limit of validity of the present theory in terms of the main system parameters? As mentioned above, the theory, derived from hydrodynamics, rests on one major assumption: the linearity of the fluid velocity profile. This assumption, in turn, implies that the scalar hydrodynamic variables (i.e., density and temperature) remain homogeneous in the course of time, if initially so. Such a homogeneous behavior is expected to occur if the relaxation time of the slowest inhomogeneous hydrodynamic mode, generated by the piston motion, does not exceed half of the period of oscillations. This general argument leads to an inequality, imposing a limiting value for the ratio of the piston to fluid mass above which the theory is expected to be valid. The predicted value for this ratio is in good agreement with all our observations in MD simulations.

It is important to recall that the present theory's derivation rests mainly on physical arguments. More precisely, we started with an assumption, examined the consequences of this assumption, and then derived the physical conditions under which those consequences are expected to be valid. Of course, we have used extensive MD simulations to check, step by step, all the details of the theory. Nevertheless, no matter how plausible, we do not yet have a mathematical proof of the validity of our main assumption, i.e., the linear fluid velocity profile assumption. A complete mathematical justification of this assumption requires an appropriate asymptotic expansion of the hydrodynamic equations in the limit of large piston mass. So far, we have not been able to achieve this goal with the required mathematical rigor.

Finally, one may ask whether the present theory can be extended to include the long-time scale relaxation toward thermodynamic equilibrium. The dynamics of that regime are dominated by the fluctuation-driven heat transfer due to the piston's Brownian motion. While there is no fluctuation source in conventional hydrodynamics, the question arises as to whether Landau-Lifshitz fluctuating hydrodynamics [19] could be used to describe this regime. At present, we do not have a clear answer to this question. The fluctuating hydrodynamic equations are much more difficult to handle analytically than their deterministic forms, but numerical techniques are known [29]. The main difficulty with this approach is the numerical instability that occurs if energy conservation is not rigorously imposed in the scheme designed to integrate the fluctuating hydrodynamic equations (recall that the global system is thermally isolated). This problem proves to be quite delicate to handle, mainly because of the moving boundary conditions, but work in this direction is in progress.

APPENDIX A

We start with the continuity equation (1), focusing first on the left compartment. Using the explicit form of the velocity (15), one finds

$$\frac{\partial \rho_L}{\partial t} = -\rho_L \frac{v_p}{X_p} - v_p \frac{x}{X_p} \frac{\partial \rho_L}{\partial x}. \tag{A1}$$

Let

$$\rho_L(x,t) = \frac{mN}{2X_p(t)L_y} \hat{\rho}_L(x,t). \tag{A2}$$

Clearly,

$$\frac{1}{X_p(t)} \int_0^{X_p(t)} \hat{\rho}_L(x,t) dx = 1, \tag{A3}$$

which simply expresses the conservation of the fluid mass in the left compartment. Inserting (A2) into (A1), one gets

$$\frac{\partial \hat{\rho}_L(x,t)}{\partial t} = -v_p \frac{x}{X_p} \frac{\partial \hat{\rho}_L}{\partial x}. \tag{A4}$$

The general solution of this equation reads (recall that $v_p = dX_p/dt$)

$$\hat{\rho}_L(x,t) = F\left(\frac{x}{X_p(t)}\right), \tag{A5}$$

where F is an arbitrary function satisfying initial and boundary conditions. In particular, since initially the system is homogeneous,

$$\hat{\rho}_L(x,t=0) = F\left(\frac{x}{X_p(0)}\right) = \text{const}, \tag{A6}$$

which, using the mass conservation relation (A3), implies that

$$\hat{\rho}_L(x,t) = 1. \tag{A7}$$

Straightforward calculations lead to the same conclusion for the right compartment, so

$$\rho_L(t) = \frac{mN}{2L_y X_p(t)}, \quad \rho_R(t) = \frac{mN}{2L_y[L_x - X_p(t)]}. \tag{A8}$$

We thus conclude that at this level of approximation (linear velocity profile) the density of the fluid remains homogeneous in time, if initially so.

APPENDIX B

The total energy of the system reads

$$E = L_y \int_0^{X_p} \left(\frac{1}{2}\rho_L v_L^2 + \rho_L e_L\right) dx + L_y \int_{X_p}^{L_x} \left(\frac{1}{2}\rho_R v_R^2 + \rho_R e_R\right) dx$$
$$+ \frac{1}{2} M v_p^2, \tag{B1}$$

where ρe is the internal energy density of the fluid. Since the total energy is conserved, its time derivative is zero. Using the explicit expressions of velocity (15) and density (16) to evaluate the integral over the space of the fluid kinetic energy, one finds

$$0 = L_y \frac{\partial}{\partial t}\left(\int_0^{X_p} \rho_L e_L dx + \int_{X_p}^{L_x} \rho_R e_R dx\right) + \left(M + \frac{mN}{3}\right)v_p \frac{dv_p}{dt}. \tag{B2}$$

Using the thermodynamic relation

$$de = c_v dT + \left[P - T\left(\frac{\partial P}{\partial T}\right)_\rho\right]\frac{d\rho}{\rho^2}, \tag{B3}$$

one obtains from (1) and (3)

$$\frac{\partial \rho e}{\partial t} = -\frac{\partial}{\partial x} v\rho e - P\frac{\partial}{\partial x} v + \frac{\partial}{\partial x} \kappa \frac{\partial}{\partial x} T + \Gamma\left(\frac{\partial v}{\partial x}\right)^2, \tag{B4}$$

where $\Gamma = \zeta + \eta$. Given the boundary conditions (5), it then follows that

$$\frac{\partial}{\partial t} \int_0^{X_p} \rho_L e_L dx = v_p \rho_L e_L|_{x=X_p} + \int_0^{X_p} \frac{\partial}{\partial t}(\rho_L e_L)dx,$$

$$= -\bar{P}_L v_p + \bar{\Gamma}_L \frac{v_p^2}{X_p} \tag{B5}$$

whereas

$$\frac{\partial}{\partial t} \int_{X_p}^{L_x} \rho_R e_R dx = -v_p \rho_R e_R|_{x=X_p} + \int_{X_p}^{L_x} \frac{\partial}{\partial t}(\rho_R e_R)dx$$

$$= +\bar{P}_R v_p + \bar{\Gamma}_R \frac{v_p^2}{L_x - X_p}, \tag{B6}$$

where $\bar{P}$ and $\bar{\Gamma}$ stand for the space average of P and Γ, respectively. Inserting (B5) and (B6) into (B2), one readily finds

$$M\left(1 + \frac{mN}{3M}\right)\frac{dv_p}{dt} = L_y(\bar{P}_L - \bar{P}_R) - L_y v_p\left(\frac{\bar{\Gamma}_L}{X_p} + \frac{\bar{\Gamma}_R}{(L_x - X_p)}\right). \tag{B7}$$

APPENDIX C

We start with the hydrodynamic equation for temperature (3) and recall that the density is homogeneous but remains a function of time through the piston position $X_p(t)$ [cf. Eq. (16)]. One may thus write the function $\phi(n)$, defined in (7), as $\phi(n) = \hat{\phi}(X_p)$. Furthermore, as discussed in Sec. III, the transport coefficients are assumed to depend only on the

"global" space averaged state variables, and not on their local values. To avoid cumbersome notations, we shall write them as a function of time, using their very same symbols. For instance, $\Gamma = \Gamma(\rho(t), \bar{T}(t)) \equiv \Gamma(t)$, where $\bar{T}(t)$ stands for the spatial average (homogeneous) temperature.

Using the explicit form of the velocity (15) and density (16) and noticing that for a two-dimensional Enskog gas $c_v = k_B/m$, the temperature equation for the left compartment (we drop the subscript "L") reads

$$\frac{\partial T}{\partial t} = -x \frac{v_p}{X_p} \frac{\partial}{\partial x} T - T \frac{v_p}{X_p} \hat{\phi}(X_p) + \frac{2L_y}{k_B N}\left(X_p \frac{\partial}{\partial x} \kappa \frac{\partial}{\partial x} T + \frac{\Gamma(t)}{X_p} v_p^2\right).$$

(C1)

To solve this equation, we first define the function Φ as

$$\Phi(t) = \int_{X_p(0)}^{X_p(t)} \frac{\hat{\phi}(\zeta)}{\zeta} d\zeta$$

(C2)

so that $\Phi(t=0)=0$. We next introduce the auxiliary function $\theta(x,t)$,

$$T(x,t) = e^{-\Phi(t)}\left(\theta(x,t) + \frac{2L_y}{k_B N}\int_0^t dt' \frac{\Gamma(t')}{X_p(t')} v_p^2(t') e^{\Phi(t')}\right).$$

(C3)

Obviously, $\theta(x,t)$ obeys the same initial and boundary conditions as $T(x,t)$, i.e.,

$$\theta(x,t=0) = T_0, \quad \left(\frac{\partial \theta}{\partial x}\right)_{x=0} = \left(\frac{\partial \theta}{\partial x}\right)_{x=X_p(t)} = 0.$$

(C4)

Inserting (C3) into (C1), one readily finds

$$\frac{\partial \theta}{\partial t} = -x \frac{v_p}{X_p} \frac{\partial}{\partial x} \theta + \frac{2L_y}{k_B N} X_p \frac{\partial}{\partial x} \kappa \frac{\partial}{\partial x} \theta.$$

(C5)

We finally proceed to the change of variable

$$\xi = \frac{x}{X_p(t)}, \quad 0 \leq \xi \leq 1.$$

(C6)

Using the chain rule, and recalling that $v_p = dX_p/dt$, one obtains

$$\frac{\partial \theta(\xi,t)}{\partial t} = \frac{2L_y}{k_B N} \frac{\partial}{\partial \xi} \frac{\kappa}{X_p(t)} \frac{\partial}{\partial \xi} \theta(\xi,t)$$

(C7)

with initial and boundary conditions [cf. Eq. (C4)]

$$\theta(\xi,t=0) = T_0, \quad \left(\frac{\partial \theta(\xi,t)}{\partial \xi}\right)_{\xi=0} = \left(\frac{\partial \theta(\xi,t)}{\partial \xi}\right)_{\xi=1} = 0.$$

(C8)

The result (C7) shows that θ obeys a heat equation in an adiabatically closed vessel. Therefore, if θ is uniform initially, then it remains so in the course of time. In particular, if $\theta(t=0)=T_0$, then $\theta(t)=T_0$, for all time.

We thus arrive at the conclusion that, within the linear velocity assumption, both the density and the temperature (and thus the pressure) remain spatially homogeneous in the course of time, if initially so. In particular, the temperature equation takes the following simple form

$$\frac{\partial T}{\partial t} = -T \frac{v_p}{X_p} \hat{\phi}(X_p) + \frac{2L_y}{k_B N} \frac{\Gamma(t)}{X_p} v_p^2.$$

(C9)

Replacing $\theta(x,t)$ by T_0 in the relation (C3), one obtains

$$T(x,t) = e^{-\Phi(t)}\left(T_0 + \frac{2L_y}{k_B N}\int_0^t dt' \frac{\Gamma(t')}{X_p(t')} v_p^2(t') e^{\Phi(t')}\right).$$

(C10)

Since $\Gamma(t) = \Gamma(T(t))$, this expression is just a convenient way of writing the equation (C9). On the other hand, the last term in (C10) represents the viscous heating effect and can be neglected for the case of a large piston mass since it is proportional to the square of the piston velocity. With this assumption,

$$T(t) = T_0 e^{-\Phi(t)}.$$

(C11)

[1] H. B. Callen, *Thermodynamics* (Wiley, New York, 1960), p. 321.

[2] R. P. Feynman, *The Feynman Lectures on Physics -Volume I*, edited by Richard P. Feynman, Robert B. Sands, and Matthew Sands, (Addison-Wesley, Reading, Massachusetts, 1963), Chap. 39.

[3] D. W. Jepsen, J. Math. Phys. **6**, 405 (1965); J. L. Lebowitz and J. K. Percus, Phys. Rev. **155**, 122 (1967); J. Piasecki and Ya. G. Sinai, "A Model of Non-Equilibrium Statistical Mechanics," Proceedings from NASI *Dynamics: Models and Kinetic Methods for Nonequilibrium Many-Body Systems* (Kluwer, Leiden, 2000).

[4] E. H. Lieb and J. Yngvason, Phys. Rep. **310**(1), 1-96 (1999); E. H. Lieb, Physica A **263**, 491 (1999); J. Piasecki and Ch. Gruber, *ibid.* **265**, 463 (1999); Ch. Gruber and J. Piasecki, *ibid.* **268**, 412 (1999).

[5] Ch. Gruber and L. Frachebourg, Physica A **272**, 392 (1999); Ch. Gruber, S. Pache, and A. Lesne, J. Stat. Phys. **108**, 669 (2002); Ch. Gruber and S. Pache, Physica A **314**, 345 (2002).

[6] N. I. Chernov and J. L. Lebowitz, J. Stat. Phys. **109**, 507 (2002); E. Caglioti, N. I. Chernov, and J. L. Lebowitz, Nonlinearity **17**, 897 (2004).

[7] E. Kestemont, C. Van den Broeck, and M. Malek Mansour, Europhys. Lett. **49**, 143 (2000).

[8] P. Reimann, Phys. Rep. **361**, 1 (2002).

[9] J. M. R. Parrondo and P. Espagnol, Am. J. Phys. **64**, 1125 (1996); C. Van den Broeck, M. Malek Mansour, and E. Kestemont, Europhys. Lett. **56**, 771 (2001).

[10] L. D. Landau and E. M. Lifshitz, *Statistical Physics* (Pergamon Press, Oxford, 1984), Vol. 1.

[11] H. B. Callen, *Thermodynamics and an Introduction to Thermostatistics* (Wiley, New York, 1985).

[12] H. S. Leff, Am. J. Phys. **62**, 120 (1994); Ch. Gruber, Eur. J. Phys. **20**, 259 (1999).

[13] B. Crosignani and P. Di Porto, Europhys. Lett. **53**, 290 (2001).

[14] Ya. G. Sinai, Theor. Math. Phys. **125**, 1351 (1999); A. I. Neishtadt and Ya. G. Sinai, J. Stat. Phys. **116**(1-4), 815-820 (2004).

[15] R. P. Bauman, Am. J. Phys. **37**, 675 (1969).

[16] B. Crosignani, P. Di Porto, and M. Segev, Am. J. Phys. **64**, 610 (1996).

[17] T. Munakata and H. Ogawa, Phys. Rev. E **64**, 036119 (2001).

[18] M. Malek Mansour, C. Van den Broeck, and E. Kestemont, Europhys. Lett. **69**, 510 (2005).

[19] L. D. Landau and E. M. Lifshitz, *Fluid Mechanics* (Pergamon Press, Oxford, 1984).

[20] D. M. Gass, J. Chem. Phys. **54**, 1898 (1971); J. A. Barker and D. E. Henderson, Rev. Mod. Phys. **48**, 587 (1976).

[21] P. Résibois and M. De Leener, *Classical Kinetic Theory of Fluids* (Plenum, New York, 1976); M. Malek Mansour, J. W. Turner, and A. Garcia, J. Stat. Phys. **48**, 1157 (1987).

[22] N. I. Khvostov and R. A. Chernyavskaya, Fluid Dyn. **6**, 881 (1971).

[23] J. Koplik and J. Banavar, Annu. Rev. Fluid Mech. **27**, 257 (1995).

[24] M. Mareschal, M. Malek Mansour, A. Puhl, and E. Kestemont, Phys. Rev. Lett. **61**, 2550 (1988); A. Puhl, M. M. Mansour, and M. Mareschal, Phys. Rev. A **40**, 1999 (1989).

[25] Kai Kadau, Timothy C. Germann, Nicolas G. Hadjiconstantinou, Peter S. Lomdahl, Guy Dimonte, Brad Lee Holian, and Berni J. Alder, Proc. Natl. Acad. Sci. U.S.A. **101**, 5851 (2004).

[26] E. S. Oran, C. K. Oh, and B. Z. Cybyk, Annu. Rev. Fluid Mech. **30**, 403 (1998).

[27] M. Malek Mansour, F. Baras, and A. L. Garcia, Physica A **240**, 255 (1997).

[28] N. Hadjiconstantinou and A. Garcia, Phys. Fluids **13**, 1040 (2001).

[29] A. Garcia, M. Malek Mansour, G. Lie, and E. Clementi, J. Stat. Phys. **47**, 209 (1987).